CERN-TH.6269/91
DTP 91/66
LU TP 91-24

Rapidity Gaps in Higgs Production

Yu.L. Dokshitzer*
Department of Theoretical Physics, University of Lund
Sölvegatan 14A, S-223 62 Lund, Sweden

V.A. Khoze*
Centre for Particle Theory, University of Durham
Durham DH1 3LE, U.K.
and
INFN Eloisatron project

and

T. Sjöstrand
CERN — Geneva

Abstract

The possibility to discriminate different Higgs production mechanisms using a rapidity gap signature is discussed. The results of Monte Carlo calculations are presented, which show that the two processes $WW \to H$ and $gg \to H$ indeed have different event structures, but also that these differences, without special care, would be masked by other effects.

---

*On leave of absence from Institute for NuclearPhysics, St. Petersburg, Gatchina 188350, USSR

CERN-TH.6269/91
October 1991

According to our current understanding, the structure of hadron production in hard processes is determined by the colour dynamics at small distances.

The first (and still best) example of colour-related phenomena is the so-called string [1] (or drag [2]) effect in $q\bar{q}g$ events of e^+e^- annihilation, which is well established experimentally [3]. Originally the depletion of particle production in the $q\bar{q}$ angular range, compared to the qg and $\bar{q}g$ ones, was predicted as the result of the Lorentz boost of a non-perturbative string stretched from the q via the g to the $\bar{q}$ [1]. In the perturbative scenario it is a result of interference among the gluon waves radiated from the $q\bar{q}g$ emitter. In the description of the colour structure of events, the two approaches are basically equivalent up to some subtle effects (see *e.g.* Refs. [4, 5]). A rich diversity of colour drag phenomena have been discussed for high-$p_\perp$ hadronic collisions, see *e.g.* Refs. [4, 6, 7, 8, 9]. One of the simplest examples is prompt γ (or W, or Z) production at large $p_\perp$ [7, 8, 9].

In the current paper we will consider the differences in colour flow structure that exist between two main Higgs production mechanisms, $WW \to H$ and $gg \to H$, see Fig. 1. In the former process, no colour exchange is involved, wherefore one expects the quasi-diffractive proton remnant states to be separated by a central rapidity gap. Not so in the $gg \to H$ case, where the two outgoing remnants are colour-connected with each other. This example was first discussed in Ref. [6], and (independently) first included in a full-fledged event simulator framework in the PYTHIA program [10]. With the help of PYTHIA we will here try to give a realistic appraisal of the size of expected differences between $WW \to H$ and $gg \to H$.

It should from the onset be made clear that an experimental study of these effects at future hadron colliders will not be easy, and maybe impossible, even after the Higgs has been found. However, the concept addressed here could find applications in a number of different other production processes, like new heavy quarks and leptons, supersymmetric particles, *etc.* One simple example is the production of a single top by the exchange of a W in the t-channel, where no colour exchange is involved, contrary to the standard $gg \to t\bar{t}$ process.

In the continued investigations, we will assume that the H is observed in the "gold-plated" channel $H \to ZZ \to 4$ leptons, as is expected to be the case when $m_H \gtrsim 150$ GeV [11, 12]. The Higgs decay products can therefore trivially be removed. Events have been generated with PYTHIA for 200 and 500 GeV Higgs masses at 16, 40 and 100 TeV pp collisions. Each run consists of 10,000 $WW \to H$ events and equally many $gg \to H$ ones, with curves normalized per event of the given type. The EHLQ set 1 structure functions [13] have been used for the figures shown, but similar results were obtained with the more recent Morfín-Tung structure functions [14]. More precisely, the absolute cross-sections, and even the relative $WW \to H$ / $gg \to H$ event composition, do depend somewhat on the choice of structure functions (at the 20–30% level), but the properties of the events themselves are but little affected.

To illustrate the difference in colour flow structure, Fig. 2 presents the "string density" in rapidity, where the extent of each string is defined by the rapidity range spanned between a colour triplet charge (q or $\overline{qq}$) and an antitriplet one ($\bar{q}$ or qq). In the $WW \to H$ process, two strings are stretched, each between a q and a qq belonging to the same original proton, and one observes that these two strings rarely extend to central rapidities. In the $gg \to H$ process, the colour exchange in the hard interaction again leads to two strings, but now with each stretched between the q of one p and the qq of the other — both strings therefore span central rapidities. The details of the behaviour at large rapidities are sensitive to the assumed structure of the proton remnants, and will not concern us here. At central rapidities the expected difference between the two scenarios is clearly

visible, however.

In the perturbative picture the depopulation of the central region in the WW case is the result of the coherent cancellation of the gluon emission at large angles ($\Theta > \Theta_s \sim m_H/E$) off the initial and final partons. In the gg case, where there is a colour octet transfer in the t-channel, the effective emission off the t-channel gluons fill the would-be rapidity gap, see Ref. [6].

Of course, the results in Fig. 2 are only illustrative, and not experimentally observable. One must include the effects of QCD cascades related to the basic hard process, and of hadronization. In Fig. 3 we show the results in terms of the (observable) charged (true) rapidity distribution, dn_{ch}/dy. The original difference is still there, although significantly reduced. The main cause is that the quarks that emit the W:s typically recoil with a transverse momentum of order m_W, and therefore appear in the final state as jets of fairly high multiplicity.

As can be seen, the size of the dip in the $WW \rightarrow H$ channel is increased for heavier Higgs masses. Further, the rapidity distance between the two peaks is increased when the CM energy is increased, although the variation is not dramatic.

However, we must confess that the scenario described above still is too optimistic, and has to be taken with a pinch of salt. A number of complications will arise in a realistic study.

1. Event rates are small, especially if one only wants to make use of the "gold-plated" events, as assumed above (to avoid contamination of the rapidity gap from the Higgs decay products).
2. With our current expectations for the top mass, the $gg \rightarrow H$ channel is expected to dominate (by a factor of five or more) above $WW \rightarrow H$, unless the Higgs is very heavy. The dip will therefore hardly be visible in the inclusive event sample.
3. Even if the hard process in $WW \rightarrow H$ does not involve a colour exchange, additional semihard or soft interactions could take place in the same event, and lead to a filling-up of the gap. This complication will be studied further below.
4. Because of the expected high luminosities of future pp colliders, several different pp events could be registered in the same bunch crossing (pileup events). Qualitatively, experimental consequences are similar to those of point 3 above, while the quantitative importance depends strongly on the luminosity.

The presence of several independent parton-parton interactions in the same event is not clearly experimentally established — AFS claims a signal [15] while UA2 fails to find a statistically significant one [16] . However, both these studies considered only the production of high-$p_\perp$ jets, while most parton interactions are expected to be fairly soft. We will therefore use the preferred multiple interaction scenario in Ref. [17] as a model for what might happen — possibly somewhat pessimistic, but not necessarily unrealistic.

With multiple interactions added, the dip in $WW \rightarrow H$ is almost gone, especially for a low-mass Higgs, Figs. 4a and 4b. While the original difference between $WW \rightarrow H$ and $gg \rightarrow H$ is preserved in absolute numbers, the relative difference is clearly now unobservable. The situation can be improved if one notes that particle production from the additional interactions is concentrated at small transverse momenta (the same holds for pileup events). If particles below $p_\perp = 2$ GeV are disregarded, a dip is indeed recovered, Fig. 4c. Alternatively, one may consider the calorimetric transverse energy flow, Fig. 4d.

A $p_\perp = 2$ GeV cutoff on charged particles is fairly optimal for separation of the two processes. This is illustrated in Fig. 5, where the total numbers of charged particles in $|y| < 2$ is shown for several different $p_\perp$ cuts. In Fig. 5a there is no $p_\perp$ cut, and therefore both distributions have long tails due to multiple interactions. As a $p_\perp$ cut is introduced,

the multiple interaction background is reduced, and then the $WW \to H$ distribution is visibly narrower than the $gg \to H$ one, in particular in terms of how often the rapidity range is completely empty, Figs. 5b and 5c. If $p_\perp$ cuts larger than 2 GeV are used, also the $gg \to H$ process has a non-negligible probability of containing no particles at all in $|y| < 2$, and separation is again decreased, Fig. 5d.

Even with the central dip gone in the inclusive sample of events, due to preponderance of the $gg \to H$ production mechanism, it could be possible to find evidence for a dip in the $WW \to H$ events. For this purpose it would be necessary to use some other, conventional, way of discrimination, *e.g.* the presence of high-$p_\perp$ jets at large rapidities in the $WW \to H$ channel [12].

In conclusion, let us emphasize that at high energies an intimate connection is expected between the event structure and the underlying production mechanism. In some sense the portrait of the event could be considered as a real partonometer making traceable the basic interaction processes.

A promising possibility to discriminate different production mechanisms is to use the specifics of the event portraits, *e.g.* , rapidity gap signatures. We considered here as one of the simplest examples the difference between the event structure in the case of the heavy Higgs boson production via gg and WW fusion.

The idea of using the rapidity gap signatures could be applied for exploration of a wide class of physical problems (*e.g.* for studying Pomeron physics), see Ref. [18] where, in particular, applications for SSC are discussed.

Acknowledgements
One of the authors (V.K.) is indebted to J.D. Bjorken and L. Cifarelli for useful discussions.

References

[1] B. Andersson, G. Gustafson and T. Sjöstrand, Phys. Lett. **94B** (1980) 211;
B. Andersson, G. Gustafson, G. Ingelman and T. Sjöstrand, Phys. Rep. **97** (1983) 31

[2] Ya.I. Azimov, Yu.L. Dokshitzer, V.A. Khoze and S.I. Troyan, Phys. Lett. **165B** (1985) 147; Sov. Jour. Nucl. Phys. **43** (1986) 95

[3] First observation in:
JADE Collaboration, W. Bartel *et al.*, Phys. Lett. **101B** (1981) 129
For recent studies, see *e.g.* :
T. Hebbeker, plenary talk at the International Lepton-Photon Symposium and Europhysics Conference on High Energy Physics, Geneva, July 26 — August 1, 1991;
OPAL Collaboration, M.Z. Akrawy *et al.*, Phys. Lett. **B261** (1991) 334

[4] Yu.L. Dokshitzer, V.A. Khoze and S.I. Troyan, *in* Perturbative QCD, ed. A.H. Mueller (World Scientific, Singapore, 1989), p.241

[5] T. Sjöstrand *et al.*, *in* Z physics at LEP 1, eds. G. Altarelli, R. Kleiss and C. Verzegnassi, CERN 89-08, Vol. 3, p. 143;
T. Sjöstrand, *in* Z^0 Physics, Cargèse 1990, eds. M. Lévy *et al.* (Plenum Press, New York, 1991), p. 367

[6] Yu.L. Dokshitzer, V.A.Khoze and S.I. Troyan, *in* Proceedings of the 6^{th} Int. Conference on Physics in Collisions 1986, ed. M. Derrick (World Scientific, Singapore, 1987), p. 365

[7] B. Andersson, H.-U. Bengtsson and G. Gustafson, Lund Preprint LU TP 82-10 (1982)

[8] R.K. Ellis, G. Marchesini and B.R. Webber, Nucl. Phys. **B286** (1987) 643

[9] Yu.L. Dokshitzer, V.A. Khoze, A.H. Mueller and S.I. Troyan, Rev. Mod. Phys. **60** (1988) 373

[10] H.-U. Bengtsson and T. Sjöstrand, Computer Physics Commun. **46** (1987) 43

[11] S. Dawson, J.F. Gunion, H.E. Haber and G.L. Kane, The Higgs Hunter's Guide (Addison-Wesley, 1990)

[12] See Higgs physics section, *in* Large Hadron Collider Workshop, eds. G. Jarlskog and D. Rein, CERN 90-10 (1990), Vol. II

[13] E. Eichten, I. Hinchliffe, K. Lane and C. Quigg, Rev. Mod. Phys. **56** (1984) 579; **58** (1985) 1065

[14] J.G. Morfín and W.-K. Tung, FERMILAB-PUB-90/74 (1990)

[15] AFS Collaboration, T. Åkesson *et al.*, Z. Physik **C34** (1987) 163

[16] UA2 Collaboration, J. Alitti *et al.*, CERN-PPE/91-101 (1991)

[17] T. Sjöstrand and M. van Zijl, Phys. Rev. **D36** (1987) 2019

[18] J.D. Bjorken, SLAC-PUB-5545 (1991)

Figure Captions

Fig. 1 Hadronic Higgs boson production via
a) WW fusion, and
b) gg fusion.

Fig. 2 String density for the two different Higgs production mechanisms. The full lines correspond to gg fusion and the dashed ones to WW fusion.
a) At $\sqrt{s} = 40$ TeV for $m_H = 200$ GeV.
b) At $\sqrt{s} = 40$ TeV for $m_H = 500$ GeV.

Fig. 3 Charged particle rapidity distribution for two mechanisms of Higgs production in pp collisions. The full lines correspond to gg fusion and the dashed ones to WW fusion.
a) At $\sqrt{s} = 16$ TeV for $m_H = 200$ GeV.
b) At $\sqrt{s} = 16$ TeV for $m_H = 500$ GeV.
c) At $\sqrt{s} = 40$ TeV for $m_H = 200$ GeV.
d) At $\sqrt{s} = 40$ TeV for $m_H = 500$ GeV.
e) At $\sqrt{s} = 100$ TeV for $m_H = 200$ GeV.
f) At $\sqrt{s} = 100$ TeV for $m_H = 500$ GeV.

Fig. 4 Charged particle rapidity distributions and transverse energy flows when multiple interactions have been added according to Ref. [17]. The full lines correspond to gg fusion and the dashed ones to WW fusion.
a) Charged rapidity distributions at $\sqrt{s} = 40$ TeV for $m_H = 200$ GeV.
b) Charged rapidity distributions at $\sqrt{s} = 40$ TeV for $m_H = 500$ GeV.
c) Charged rapidity distributions for particles with $p_\perp > 2$ GeV, at $\sqrt{s} = 40$ TeV for $m_H = 500$ GeV.
d) Transverse energy flow as function of rapidity at $\sqrt{s} = 40$ TeV for $m_H = 500$ GeV.

Fig. 5 Charged particle multiplicity distribution in the rapidity range $|y| < 2$, at $\sqrt{s} = 40$ TeV for $m_H = 500$ GeV. The full lines correspond to gg fusion and the dashed ones to WW fusion.
a) For all transverse momenta.
b) For $p_\perp > 1$ GeV.
c) For $p_\perp > 2$ GeV.
d) For $p_\perp > 4$ GeV.

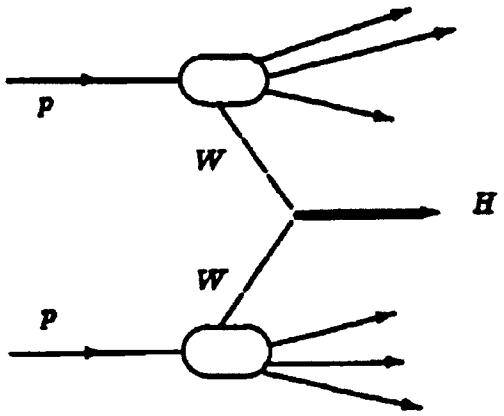

Fig. 1a

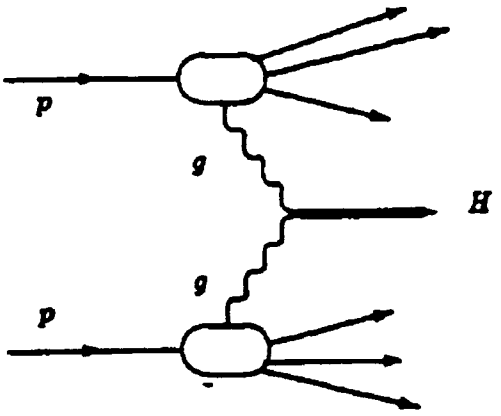

Fig. 1b

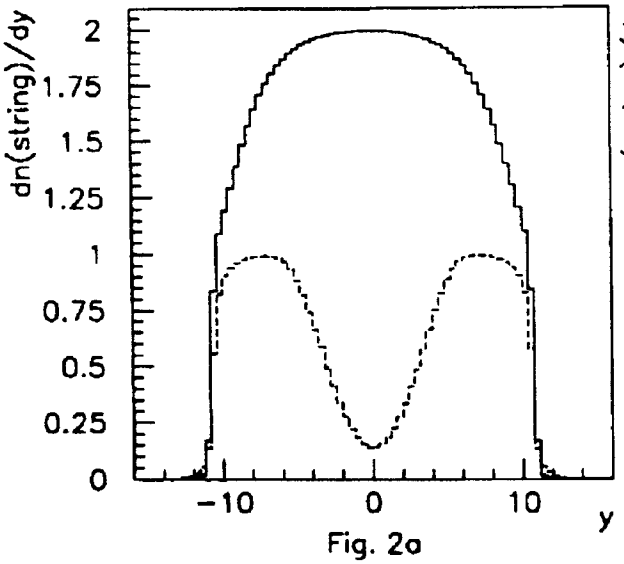

Fig. 2a

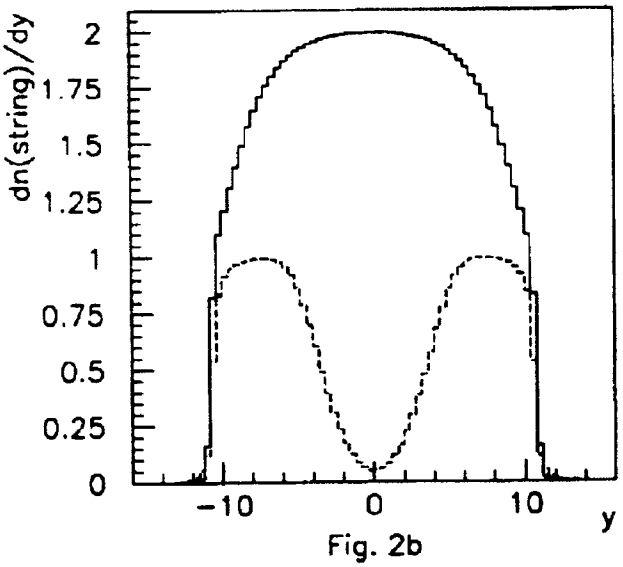

Fig. 2b

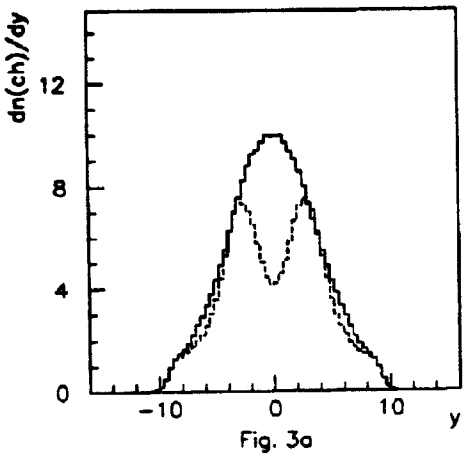

Fig. 3a

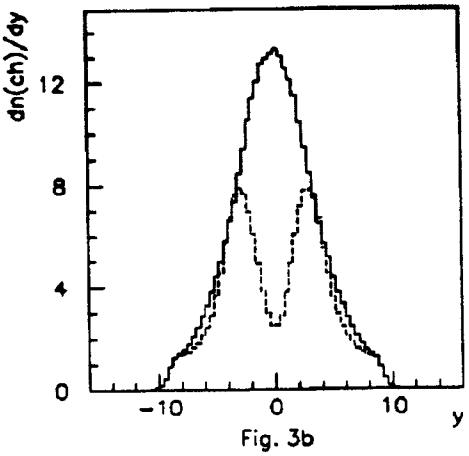

Fig. 3b

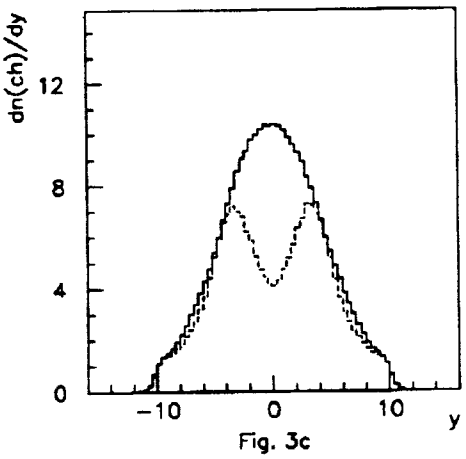

Fig. 3c

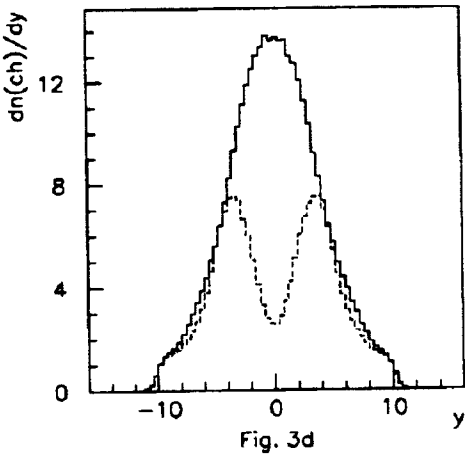

Fig. 3d

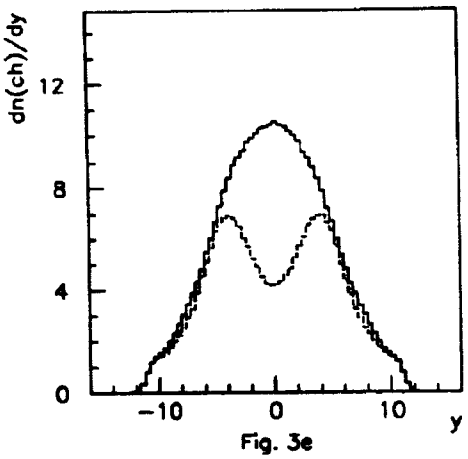

Fig. 3e

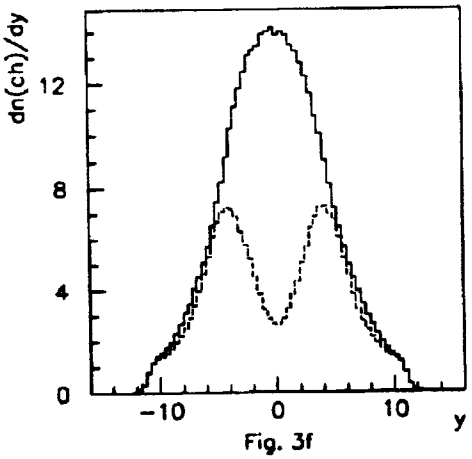

Fig. 3f

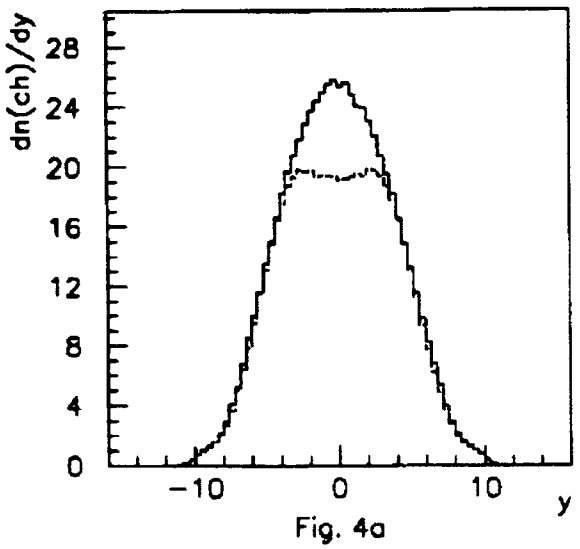

Fig. 4a

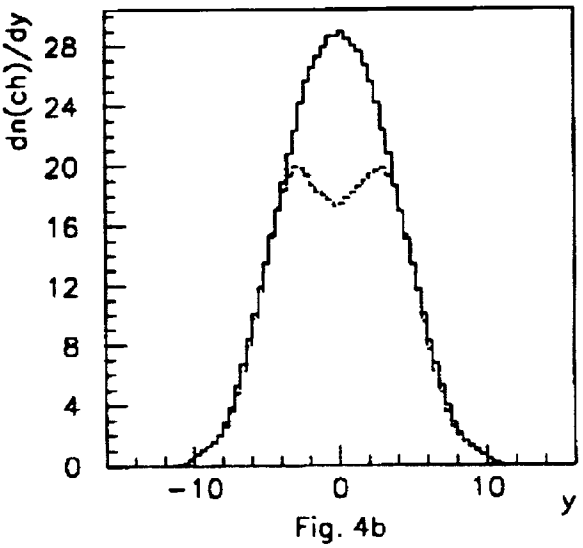

Fig. 4b

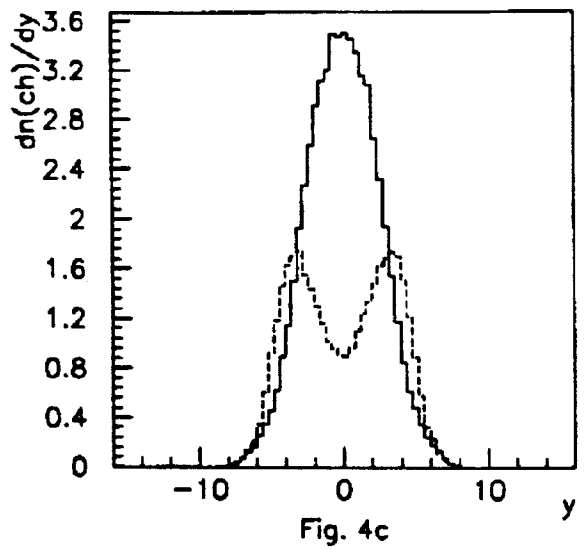

Fig. 4c

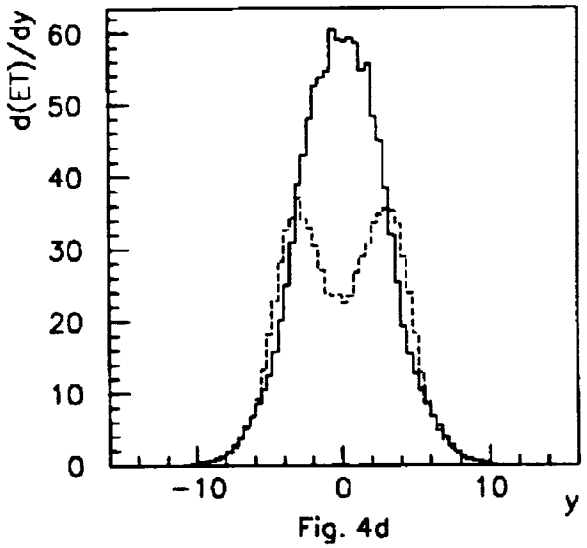

Fig. 4d

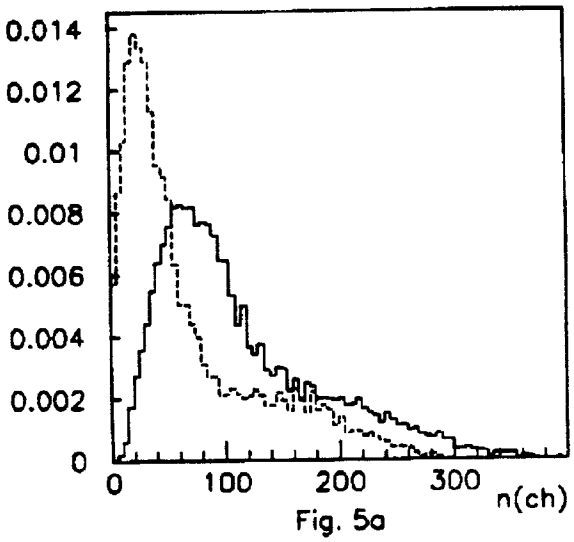

Fig. 5a

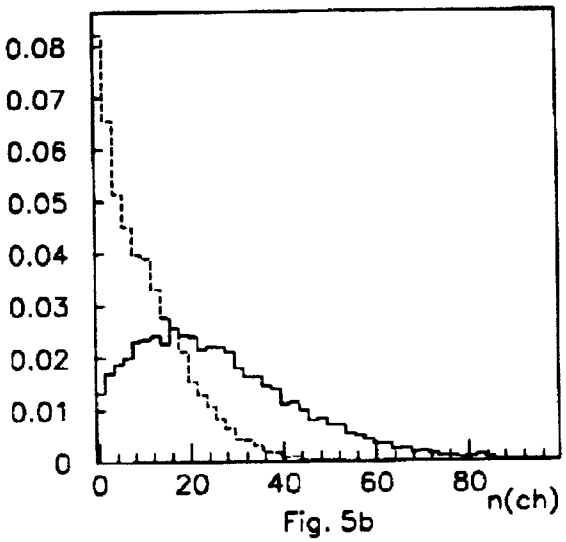

Fig. 5b

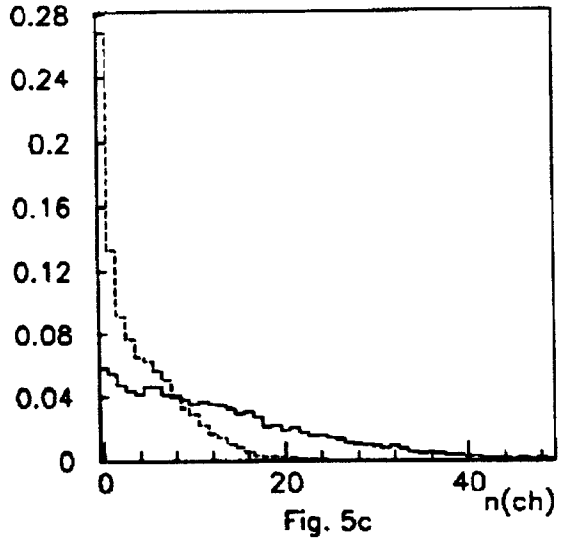

Fig. 5c

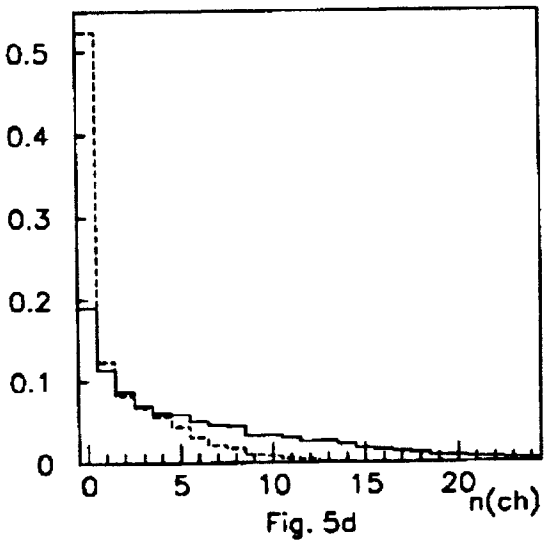

Fig. 5d